Revisiting the di-Higgs production processes at the FCC-hh

Shankha Banerjee
IPPP, Durham University

January 16, 2020

Based on

Eur. Phys. J. C (2018) 78: 322 (with C. Englert, M. Mangano, M. Selvaggi and M. Spannowsky)
Phys.Rev. D100 (2019) 073012 (with F. Krauss and M. Spannowsky)

Plan of my talk

- Motivation
- Status of the di-Higgs searches
- Di-Higgs in the EFT
- Non resonant di-Higgs production at the HL-LHC
- Di-Higgs + jet at FCC-hh
- $t\bar{t}hh$ at FCC-hh
- Summary and Outlook

Motivation

- Di-Higgs provides means to directly probe Higgs self coupling
- Indirect probe: Through radiative corrections of single Higgs productions [Goertz *et. al.*; 2013, McCullough; 2013, Degrassi *et. al.*; 2016]
- Challenging task : small di-Higgs cross-section in SM ($39.56^{+7.32\%}_{-8.38\%}$ fb at NNLO + NNLL at 14 TeV with the exact top-quark mass dependence at NLO [deFlorian *et. al.*; 2013, Borowka *et. al.*; 2016]) $\leftarrow$ partial cancellation of triangle and box diagram contributions
- LHC or 100 TeV colliders : self-coupling measurement at 10-50% precision possible $\rightarrow$ size of dataset, beam energy, control over systematics
- Assuming SM couplings, HL-LHC prediction: $-0.8 < \frac{\lambda}{\lambda_{\rm SM}} < 7.7$ at 95% C.L. [ATL-PHYS-PUB-2017-001]

Motivation

- Enhancement of σ_{hh} $\rightarrow$ *s*-channel heavy di-Higgs resonance [xSM models *etc.*] [Mühlleitner *et. al.*; 2015; Ramsey-Musolf *et. al.*; 2016 *etc.*], new coloured particles in loops [Kribs *et. al.*; 2012, Nakamura *et. al.*; 2017] or HD operators [Nishiwaki *et. al.*; 2013] $\rightarrow$ kinematics altered $\rightarrow$ requires different experimental search strategies
- Till date $\rightarrow$ major focus on BSM di-Higgs sector $\rightarrow$ enhancement in production
- New physics can affect Higgs *decays* $\rightarrow$ exotic Higgs decays now actively studied [Curtin *et. al.*; 2015]
- Worthwhile to consider exotic decays for di-Higgs $\rightarrow$ present bounds on variety of Higgs decays : BR very weak (10-50%) [SB, Batell, Spannowsky; 2016]

Di-Higgs production cross-sections as functions of $\sqrt{s}$

- Di-Higgs cross-sections [Baglio *et. al.*; 2015]

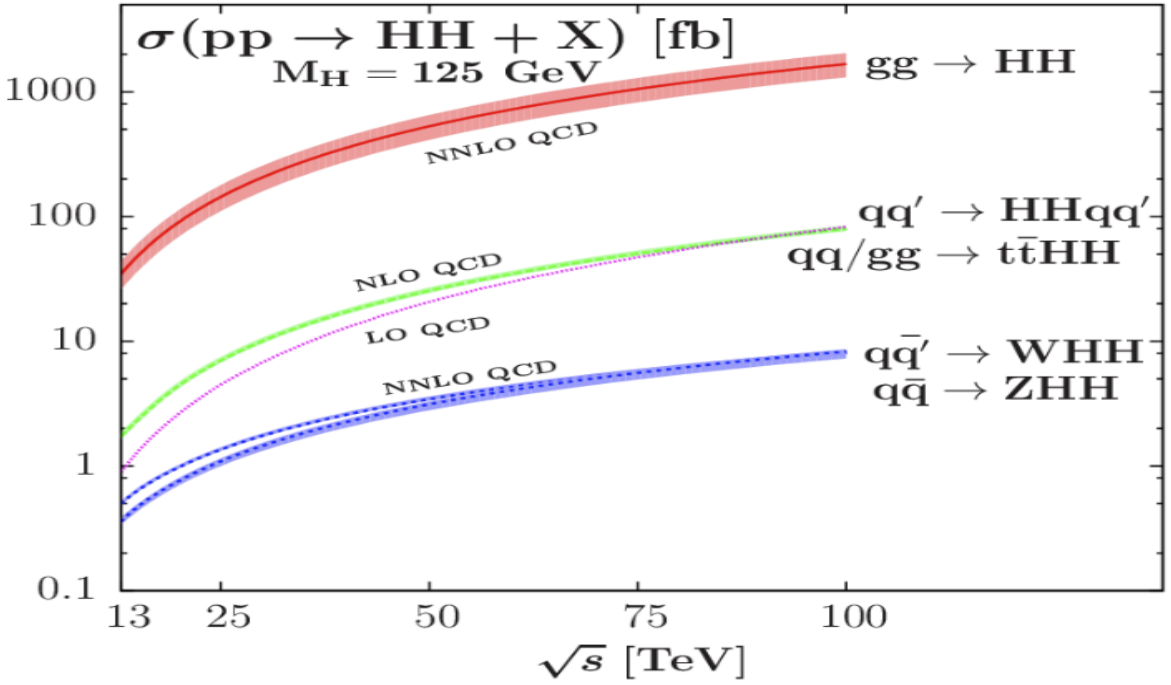

Status of the di-Higgs searches

Channel	CMS (NR) ($\times$SM)	CMS (R) [fb, (GeV)]	ATLAS (NR) ($\times$SM)	ATLAS (R) [fb, (GeV)]
$b\bar{b}b\bar{b}$	75	1500-45 (260-1200)	13	2000-2 (260-3000)
$b\bar{b}\gamma\gamma$	24	240-290 (250-900)	22	1100-120 (275-400)
$b\bar{b}\tau^+\tau^-$	30	3110-70 (250-900)	12.7	1780-100 (260-1000)
$\gamma\gamma WW^*$ ($\gamma\gamma\ell\nu jj$)			200	40000-6100 (260-500)
$b\bar{b}\ell\nu\ell\nu$	79	20500-800 (300-900)	300	6000-170 (500-3000)
WW^*WW^*			160	9300-2800 (260-500)

Table: Non-resonant (NR) and resonant (R) double Higgs production. Numbers in brackets show the range of the heavy scalar mass.

NR: Non-resonant, R: Resonant

SMEFT motivation

- Many reasons to go beyond the SM, *viz.* gauge hierarchy, neutrino mass, dark matter, baryon asymmetry etc.
- Plethora of BSM theories to address these issues
- Two phenomenological approaches:
  - *Model dependent:* study the signatures of each model individually
  - *Model independent:* low energy effective theory formalism – analogous to Fermi's theory of beta decay
- The SM here is a low energy effective theory valid below a cut-off scale Λ
- A bigger theory (either weakly or strongly coupled) is assumed to supersede the SM above the scale Λ
- At the perturbative level, all heavy ($> \Lambda$) DOF are decoupled from the low energy theory (Appelquist-Carazzone theorem)
- Appearance of HD operators in the effective Lagrangian valid below Λ

$$\mathcal{L} = \mathcal{L}_{SM}^{d=4} + \sum_{d\geq 5} \sum_{i} \frac{f_i}{\Lambda^{d-4}} \mathcal{O}_i^d$$

Relevant operators

- Dimension 6 operators which modify the Higgs self-interactions

$$\mathcal{O}_{\Phi,1} = (D_\mu \Phi^\dagger)\Phi\Phi^\dagger(D^\mu\Phi) \quad \mathcal{O}_{\Phi,2} = \frac{1}{2}\partial_\mu(\Phi^\dagger\Phi)\partial^\mu(\Phi^\dagger\Phi)$$

$$\mathcal{O}_{\Phi,3} = \frac{1}{3}(\Phi^\dagger\Phi)^3 \quad \mathcal{O}_{\Phi,4} = (D_\mu\Phi^\dagger)(D^\mu\Phi)\Phi^\dagger\Phi \quad \mathcal{O}_{GG} = G^a_{\mu\nu}G^{a,\mu\nu}\Phi^\dagger\Phi$$

- $\mathcal{O}_{\Phi,2/3}$ only modify Higgs self-couplings but $\mathcal{O}_{\Phi,1/4}$ also modify HVV couplings and V masses
- $\mathcal{O}_{\Phi,1}$ contributes to m_Z and not to m_W $\rightarrow$ Violates Custodial symmetry $\rightarrow$ Strongly constrained by T-parameter $\rightarrow$ Neglected for collider studies
- Redundancy amongst operators upon using EOMs $\rightarrow$ $\mathcal{O}_{\Phi,2}$, $\mathcal{O}_{\Phi,3}$ and $\mathcal{O}_{\Phi,4}$ are not independent
- Including SM Yukawa, the operator $\mathcal{O}_{\Phi,f} = (\Phi^\dagger\Phi)\bar{L}\Phi f_R + \mathrm{h.c.}$, where $L = (f_L^u, f_L^d)^T$ becomes relevant
- One can remove $\mathcal{O}_{\Phi,4}$ using EOMs $\rightarrow$ Left with $(\mathcal{O}_{\Phi,2}, \mathcal{O}_{\Phi,3}, \mathcal{O}_{\Phi,f}, \mathcal{O}_{GG})$

Non-linear EFT realisation

- Many popular BSM extensions which give rise to modification of Higgs interactions
- Composite Higgs models assume that the Higgs is a pNGB of a strongly coupled UV completion
- The electroweak chiral Lagrangian best describes the low-energy effects of a strongly-coupled embedding of the SM

$$\begin{aligned}\mathcal{L}^{\mathrm{ew}\chi} \supset \quad & - \quad V(h) + \frac{g_s^2}{48\pi^2} G^a_{\mu\nu} G_a^{\mu\nu} \left(k_g \frac{h}{v} + \frac{1}{2} k_{2g} \frac{h^2}{v^2} + \cdots \right) \\ & - \quad \frac{v}{\sqrt{2}} (\bar{u}^i_L \ \bar{d}^i_L) \Sigma \left[1 + c \frac{h}{v} + c_2 \frac{h^2}{v^2} + \cdots \right] \begin{pmatrix} y^u_{ij} u^j_R \\ y^d_{ij} d^j_R \end{pmatrix} + \mathrm{h.c.},\end{aligned}$$

with

$$V(h) = \frac{1}{2} m_h^2 h^2 + d_3 \frac{m_h^2}{2v} h^3 + d_4 \frac{m_h^2}{8v^2} h^4 + \cdots \ .$$

- Here the $SU(2) \times U(1)$ symmetry is non-linearly realised $\Sigma(x) = e^{i\sigma^a \phi^a(x)/v}$ with the Goldstone bosons ϕ^a (a=1,2,3) and the Pauli matrices σ^a

Non-linear EFT realisation

- 5 vertices are of imminent importance, *viz.*, k_g, k_{2g}, c, c_2, d_3 in the top-Higgs sector
- k_g and c $\rightarrow$ can be constrained from gluon-fusion, VBF, $t\bar{t}h$ production
- k_{2g}, c_2 and d_3 $\rightarrow$ can be constrained at LO from double-Higgs processes
- To over-constrain the parameter space of $\mathcal{L}^{\mathrm{ew}\chi}$ it is necessary to access as many di-Higgs processes as possible, *viz.*, $pp \rightarrow hh, hhj, hhjj, t\bar{t}hh$
- $t\bar{t}hh$ is the only process with appreciable cross-section that has the ability to constrain c_2 at tree-level
- Here however, we will discuss in terms of the following simplified Lagrangian

$$\mathcal{L}^{\mathrm{simp}} = \mathcal{L}^{SM} + (1-\kappa_\lambda)\lambda_{\mathrm{SM}} h^3 + \kappa_{t\bar{t}hh}(\bar{t}_L t_R h^2 + \mathrm{h.c.}) - \frac{1}{8}\kappa_{\mathrm{gghh}} \mathrm{G}^{\mathrm{a}}_{\mu\nu}\mathrm{G}^{\mu\nu}_{\mathrm{a}}\mathrm{h}^2,$$

where $\lambda_{\mathrm{SM}} = \lambda v = \frac{m_h^2}{2v}$ and $\kappa_\lambda = \lambda_{\mathrm{BSM}}/\lambda_{\mathrm{SM}}$

Bases translations

[Giudice, Grojean, Pomarol, Rattazzi; 2007, Feruglio; 1993]

Coupling	Non-linear EFT	Simplified Lagrangian	SILH
hhh	d_3	κ_λ	$1+(c_6-c_\tau/4-3c_H/2)\xi$
$t\bar{t}hh$	c_2	$-\frac{\sqrt{2}v}{y_t}\kappa_{t\bar{t}hh}$	$-(c_H+3c_y+c_\tau/4)\xi/2$
$gghh$	k_{2g}	$-\frac{12\pi^2 v^2}{g_s^2}\kappa_{gghh}$	$3c_g\left(\frac{y_t^2}{g_\rho^2}\right)\xi$

Table: Relationship between the hhh, $t\bar{t}hh$ and $gghh$ vertices in three different bases, where $\xi \equiv (v/f)^2$.

$$\begin{aligned}\mathcal{L}_{\rm SILH} = & \frac{\bar{c}_H}{2v^2}\partial^\mu\left[\Phi^\dagger\Phi\right]\partial_\mu\left[\Phi^\dagger\Phi\right] + \frac{\bar{c}_T}{2v^2}\left[\Phi^\dagger \overleftrightarrow{D}^\mu\Phi\right]\left[\Phi^\dagger\overleftrightarrow{D}_\mu\Phi\right] - \frac{\bar{c}_6\lambda}{v^2}\left[\Phi^\dagger\Phi\right]^3 \\ & - \left[\frac{\bar{c}_u}{v^2}y_u\Phi^\dagger\Phi\ \Phi^\dagger\cdot\bar{Q}_L u_R + \frac{\bar{c}_d}{v^2}y_d\Phi^\dagger\Phi\ \Phi\bar{Q}_L d_R + \frac{\bar{c}_l}{v^2}y_\ell\ \Phi^\dagger\Phi\ \Phi\bar{L}_L e_R + \text{h.c.}\right] \\ & + \frac{ig\ \bar{c}_W}{m_W^2}\left[\Phi^\dagger T_{2k}\overleftrightarrow{D}^\mu\Phi\right]D^\nu W^k_{\mu\nu} + \frac{ig'\ \bar{c}_B}{2m_W^2}\left[\Phi^\dagger\overleftrightarrow{D}^\mu\Phi\right]\partial^\nu B_{\mu\nu}\end{aligned}$$

Non resonant di-Higgs production at the HL-LHC

[A. Adhikary, SB, R. K. Barman, B. Bhattacherjee, S. Niyogi; 2017]

- We choose channels based on the rate and cleanliness
- Focus on final states with leptons and/or photons
- Focus on 11 channels, *viz.*
  - $b\bar{b}\gamma\gamma$
  - $b\bar{b}\tau^+\tau^- \to b\bar{b}\ell\ell + \not{E}_T,\ b\bar{b}\ell\tau_h + \not{E}_T,\ b\bar{b}\tau_h\tau_h + \not{E}_T$
  - $b\bar{b}WW^* \to b\bar{b}\ell\ell + \not{E}_T,\ b\bar{b}\ell jj + \not{E}_T$
  - $WW^*\gamma\gamma \to \ell\ell\gamma\gamma + \not{E}_T,\ \ell jj\gamma\gamma + \not{E}_T$
  - $WW^*WW^* \to \ell^\pm\ell^\pm jjjj + \not{E}_T,\ \ell\ell\ell jj + \not{E}_T,\ \ell\ell\ell\ell + \not{E}_T$
- $4\tau,\ WW^*\tau^+\tau^-,\ ZZ^*\tau^+\tau^-,\ 4\gamma,\ ZZ^*\gamma\gamma,\ 4Z$ may be important at 100 TeV colliders
- Follow CMS and ATLAS analyses (when available) and optimise upon them

Non resonant di-Higgs production at the HL-LHC: $b\bar{b}\gamma\gamma$

- $S/B = 0.19$ and $S/\sqrt{B} = 1.76\sigma$ CMS (ATLAS) projection: 1.6σ (1.05σ)

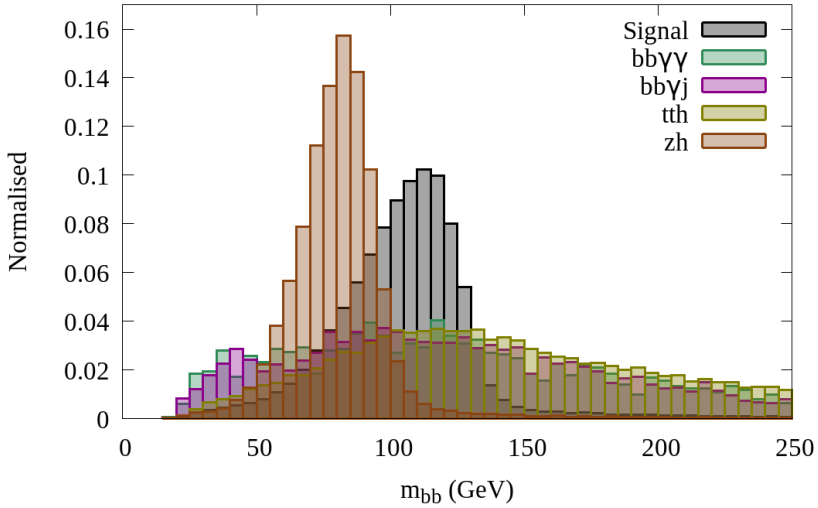

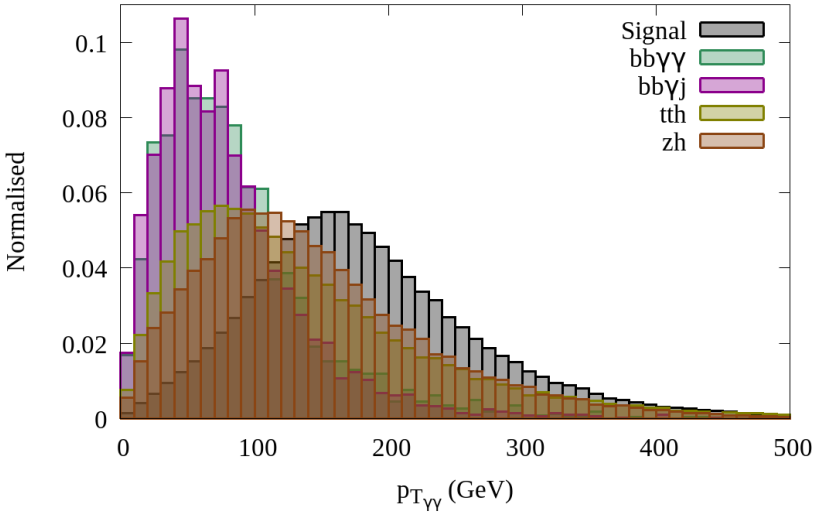

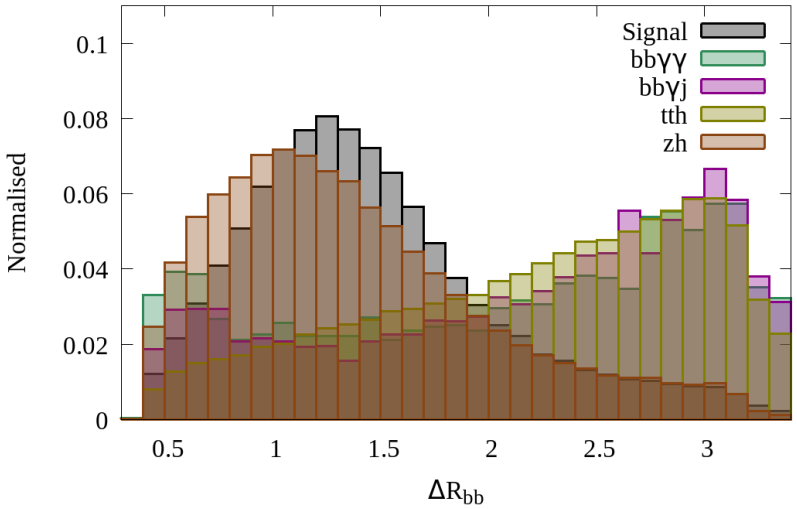

Non resonant di-Higgs production at the HL-LHC: $b\bar{b}WW^*$

- Leptonic: $S/B = 0.01$ and $S/\sqrt{B} = 0.62$; CMS projection: $S/B = 0.009$ and $S/\sqrt{B} = 0.59$

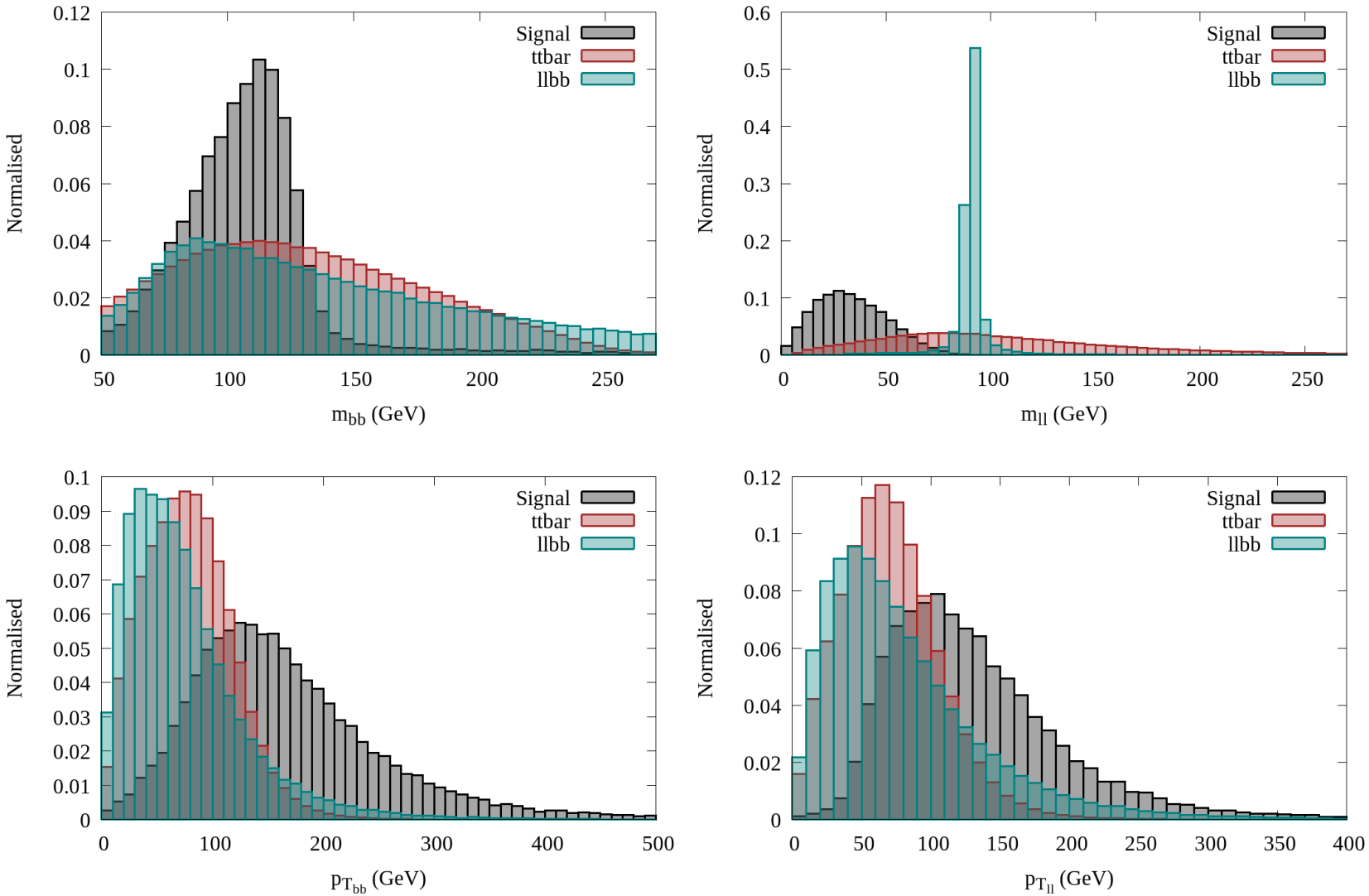

Non resonant di-Higgs production at the HL-LHC: Summary

[A. Adhikary, SB, R. K. Barman, B. Bhattacherjee, S. Niyogi; 2017]

- Bleak prospects for discovering SM non-resonant di-Higgs channel at HL-LHC with 3 ab^{-1} data
- $b\bar{b}\gamma\gamma$ is the cleanest ($S/B \sim 0.19$) but suffers from small rate
- Combined significance $\sim 3\sigma$ from the aforementioned channels
- Purely leptonic case for $b\bar{b}WW^*$ shows promise but needs better handle over backgrounds $\rightarrow$ data driven backgrounds
- Both semi-leptonic and leptonic channels for $\gamma\gamma WW^*$ show excellent S/B (0.11 and 0.4 respectively) $\rightarrow$ need larger luminosity (considering CMS and ATLAS datasets separately to form 6 ab^{-1}) or higher energy colliders

Di-Higgs + jet at FCC-hh

[SB, C. Englert, M. Mangano, M. Selvaggi, M. Spannowsky; 2018]

- Observing the Higgs self-coupling at the HL-LHC seem difficult at the moment
- Di-Higgs cross-section increases by 39 times going from 14 TeV $\rightarrow$ 100 TeV
- Extra jet emission becomes significantly less suppressed: 77 times enhancement from 14 TeV $\rightarrow$ 100 TeV collider $\rightarrow$ extra handle
- Recoiling a collimated Higgs pair against a jet exhibits more sensitivity (decorrelates $p_{T,h}$ and m_{hh}) to λ_{hhh} as compared to $pp \rightarrow hh$ $\rightarrow$ statistically limited at the LHC
- Study $hhj \rightarrow b\bar{b}\tau^+\tau^- j \rightarrow b\bar{b}\tau_h(\tau_\ell)\tau_\ell j$ and $hhj \rightarrow b\bar{b}b\bar{b}j$
- Use substructure technique: BDRS [Butterworth, *et. al.*; 2008] with mass drop and filtering

Di-Higgs + jet at FCC-hh ($jb\bar{b}\tau^+\tau^-$)

- $R = 1.5$, $p_T^j > 110$ GeV, τ-tag efficiency 70%, b-tag efficiency 70%, b-mistag rate 2%; Combined $\tau_h\tau_h$ and $\tau_h\tau_\ell$
- Backgrounds: EW (example: $HZ/\gamma^* +$ jet), QCD+EW (Example: $b\bar{b}Z/\gamma^* +$ jet), $t\bar{t}+$ jet

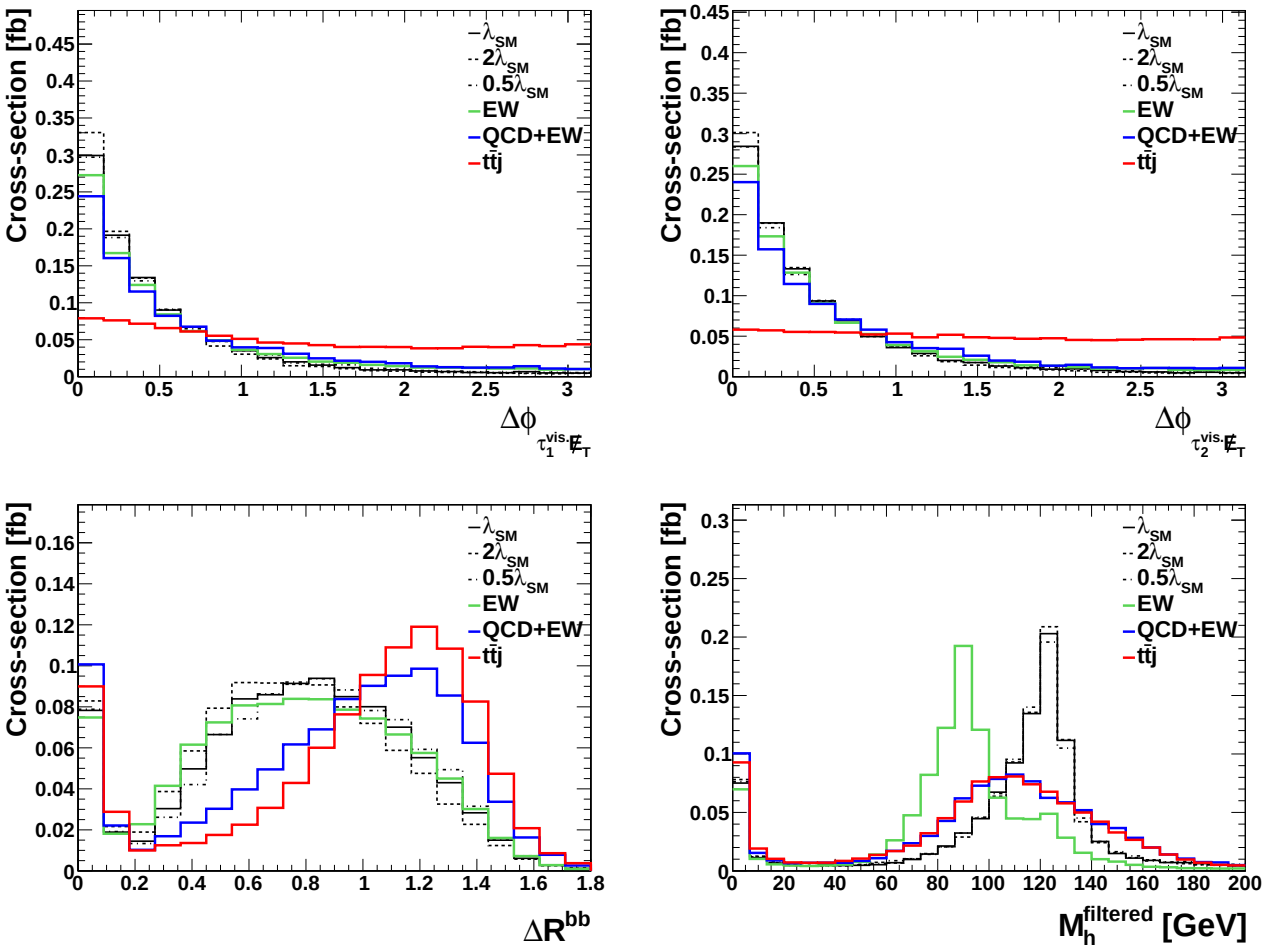

Di-Higgs + jet at FCC-hh ($jb\bar{b}\tau^+\tau^-$)

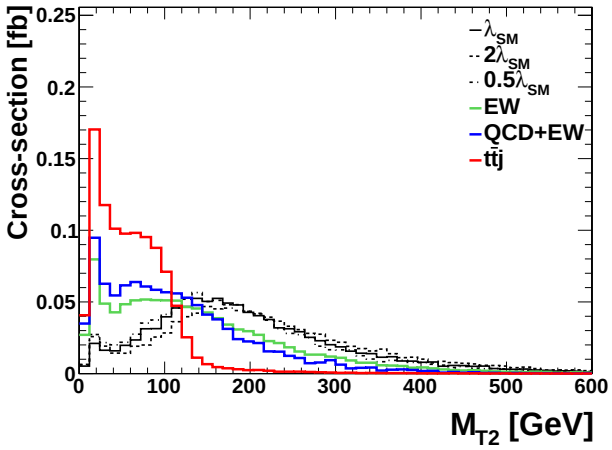

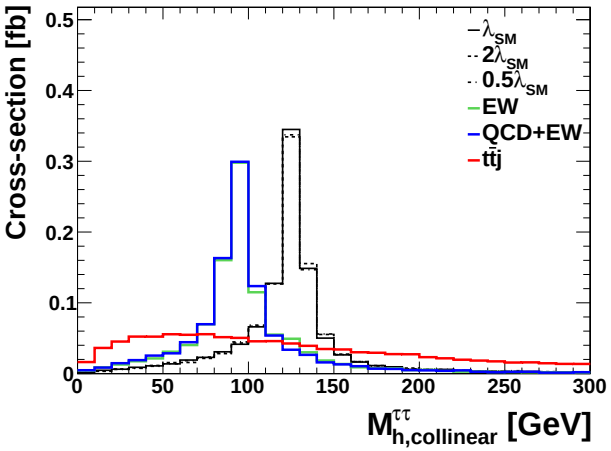

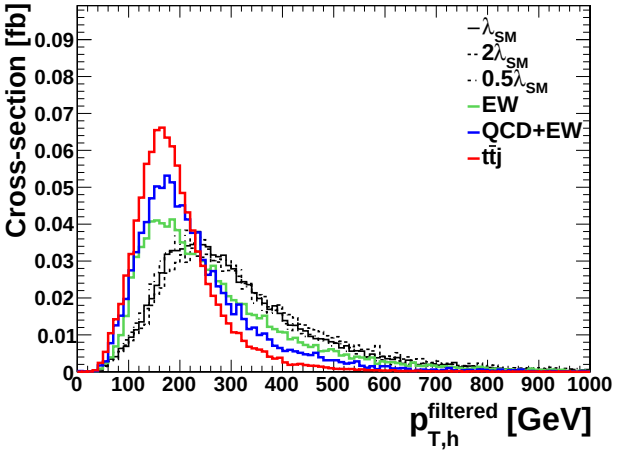

Di-Higgs + jet at FCC-hh ($jb\bar{b}\tau^+\tau^-$)

observable	reconstructed object
p_T	2 hardest filtered subjets 2 visible τ objects (τ_ℓ or τ_h) hardest non b, τ-tagged jet reconstructed Higgs from filtered jets reconstructed Higgs from visible τ final states
p_T ratios	2 hardest filtered jets 2 visible τ final state objects
m_{T2}	described before
ΔR	two hardest filtered subjets two visible τ objects ($\tau_\ell\tau_\ell$ or $\tau_\ell\tau_h$) b-tagged jets and lepton or τ_h b-tagged jets and jet j_1 lepton or τ_h with jet j_1
$M_{\tau\tau}^{\text{col}}$	collinear approximation of $h \to \tau\tau$ mass
M^{filt}	filtered j_1 and j_2 (and j_3 if present)
$M_{hh}^{vis.}$	filtered jets and leptons (or lepton and τ_h)
$\not{E}_T$	reduce sub-leading backgrounds
$\Delta\phi$	between visible τ final state objects and $\not{E}_T$ between filtered jets system and $\ell\ell$ (or $\ell\ \tau_h$) systems
N_{jets}	number of anti-k_T jets with $R = 0.4$

Di-Higgs + jet at FCC-hh ($jb\bar{b}\tau^+\tau^-$)

[SB, C. Englert, M. Mangano, M. Selvaggi, M. Spannowsky; 2018]

	signal [fb]	QCD+QED [fb]	QED [fb]	$t\bar{t}j$ [fb]	tot. background [fb]	S/B	$S/\sqrt{B}$, 30/ab
$\kappa_\lambda = 0.5$	0.428					0.121	39.44
$\kappa_\lambda = 1$	0.363	0.95	0.27	2.31	3.53	0.103	33.44
$\kappa_\lambda = 2$	0.264					0.075	24.31

$$0.76 < \kappa_\lambda < 1.28 \quad 3/\text{ab}$$

$$0.92 < \kappa_\lambda < 1.08 \quad 30/\text{ab}$$

at 68% confidence level using the CLs method.

Comparison with optimised cut-and-count analysis

cut	cross section after cut [fb]					
	$\kappa_\lambda = 1$	$\kappa_\lambda = 0.5$	$\kappa_\lambda = 2$	QCD+EW	EW	$t\bar{t}j$
preselection	0.86	1.09	0.56	11.73	2.20	4090.29
$m_{T2} > 120$ GeV	0.65	0.78	0.45	4.65	1.10	300.68
$\Delta\Phi(\tau_{\text{vis},2}, \not{E}_T) < 1.5$	0.62	0.74	0.43	4.43	1.05	196.36
100 GeV $< M_{\tau,\tau} <$ 150 GeV	0.48	0.57	0.33	0.96	0.26	28.05
$\Delta\Phi(\tau_{\text{vis},1}, \not{E}_T) < 1.5$	0.47	0.56	0.32	0.92	0.25	21.75
$\Delta R(b_1 \tau_{\text{vis},1}) > 0.8$	0.47	0.56	0.32	0.92	0.25	20.28
$p_T(H_{\tau_{\text{vis},1}\tau_{\text{vis},2}}) > 60.0$ GeV	0.45	0.53	0.31	0.88	0.24	19.02
$\Delta R(b_1 \tau_{\text{vis},2}) > 0.8$	0.44	0.52	0.31	0.87	0.24	18.91
100 GeV $< M_{\text{inv,filt}} <$ 150 GeV	0.32	0.38	0.22	0.43	0.06	5.78
$\Delta R(b_1 b_2) > 0.8$	0.32	0.38	0.22	0.43	0.06	5.46
$\Delta R(\tau_{\text{vis},1}\tau_{\text{vis},2}) > 0.8$	0.31	0.37	0.22	0.42	0.06	5.15
	0.36	0.44	0.26	0.95	0.27	2.31
BDT performance [fb]						

Di-Higgs + jet at FCC-hh ($jb\bar{b}b\bar{b}$)

- Major background: pure QCD: $g \to b\bar{b}$ (soft and collinear splittings $\to$ Resulting fat jets (R = 0.8) are one-pronged.
- Signal: $H \to b\bar{b}$; clear two prongs
- Requre: $\tau_{2,1} < 0.35$ and $100\ \mathrm{GeV} < m_{SD} < 130\ \mathrm{GeV}$

	signal	QCD	QCD+EW	EW	tot. background	$S/B \times 10^3$	$S/\sqrt{B}$, 30/ab
$\kappa_\lambda = 0.5$	0.094					20.8	7.67
$\kappa_\lambda = 1$	0.085	4.3	0.1	0.003	4.4	19.1	6.61
$\kappa_\lambda = 2$	0.071					16.2	5.85

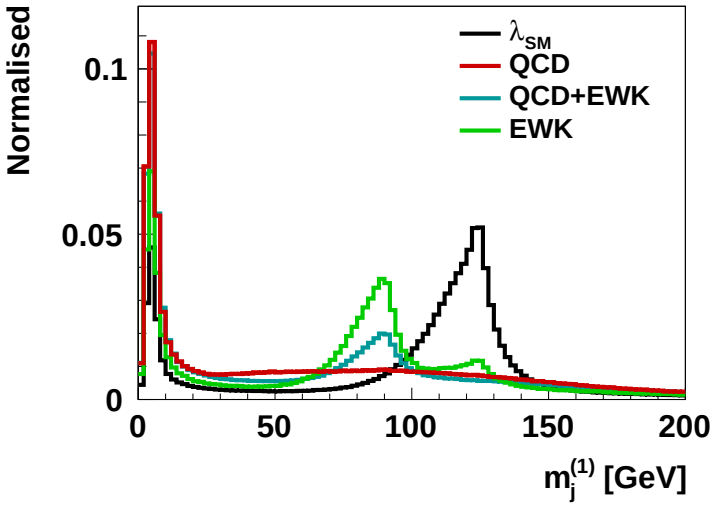

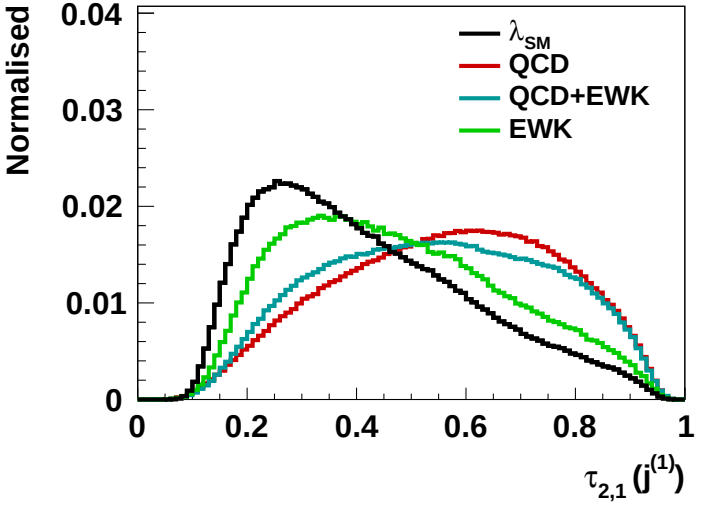

Constraining κ_λ and $\kappa_{t\bar{t}hh}$ from $t\bar{t}hh$ at 100 TeV

- Feynman diagrams showing the impact of the three effective vertices, *viz.*, hhh, $t\bar{t}hh$ and $gghh$

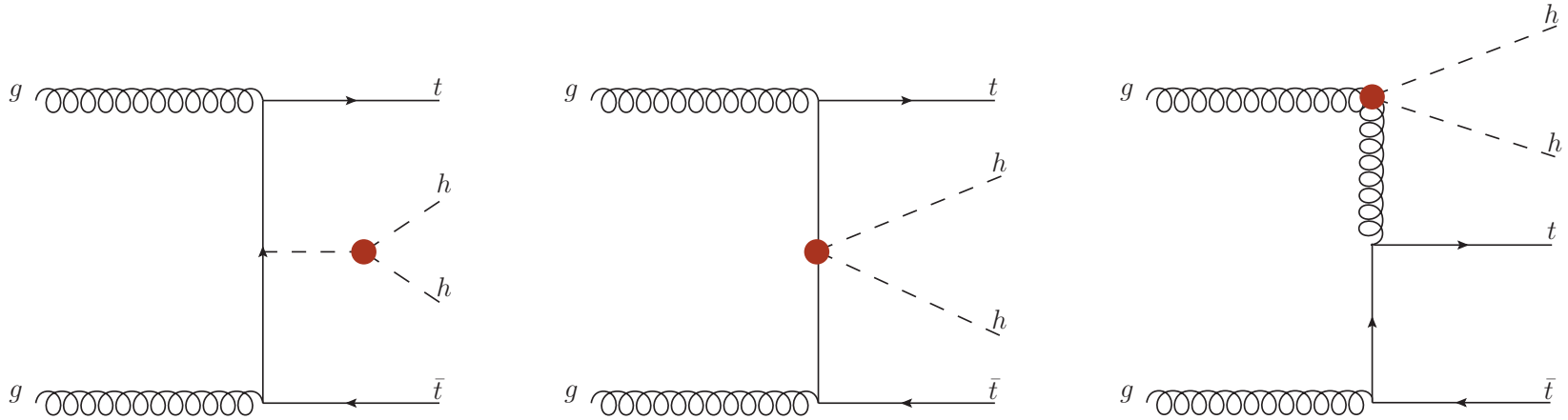

Constraining κ_λ and $\kappa_{t\bar{t}hh}$ from $t\bar{t}hh$ at FCC-hh

- σ/σ_{SM} with respect to $\kappa_\lambda, \kappa_{t\bar{t}hh}, \kappa_{gghh}$
- First row shows σ/σ_{SM} at 100 TeV and at 14 TeV [Frederix *et. al.*; 2014]

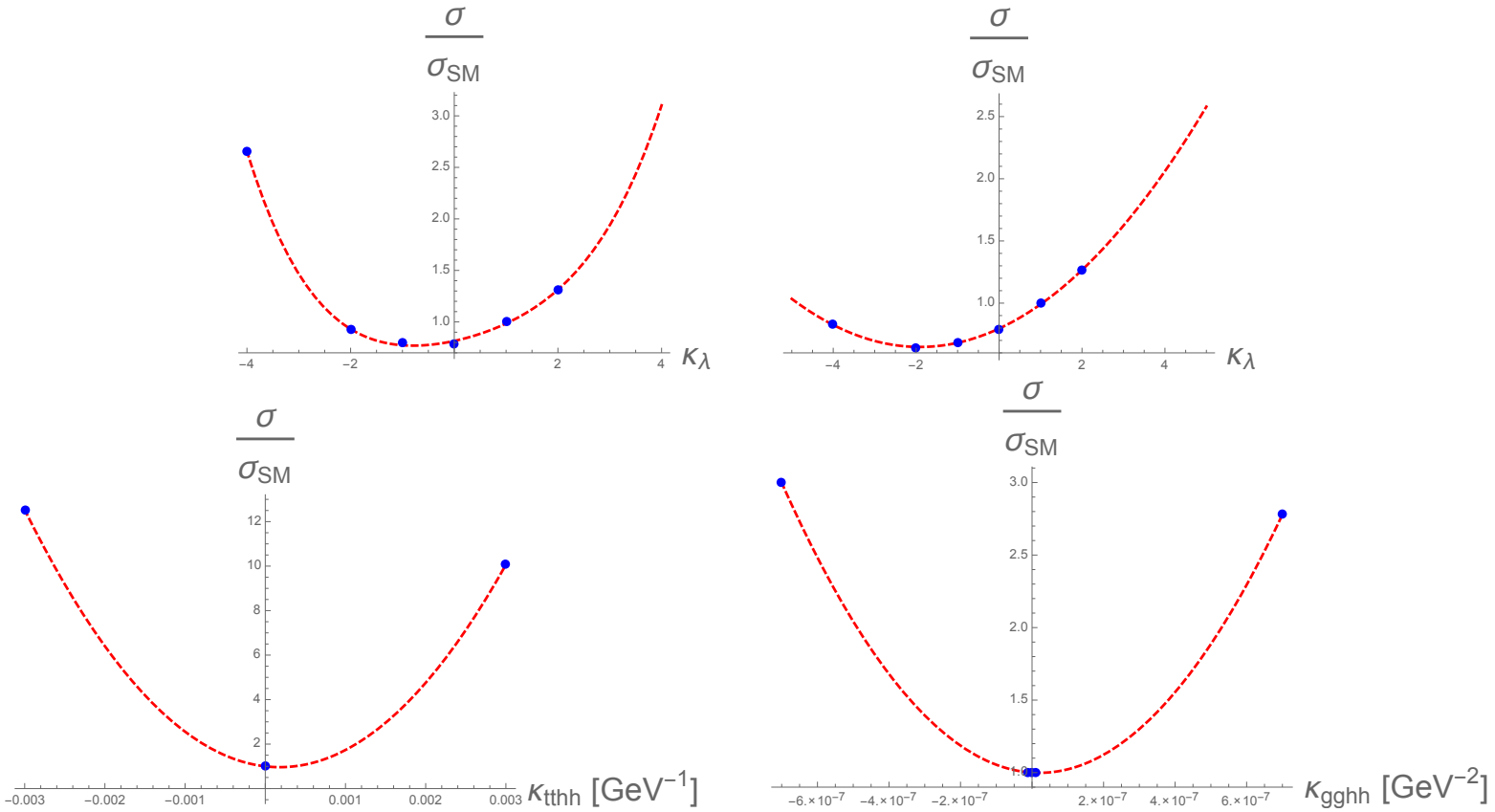

Constraining κ_λ and $\kappa_{t\bar{t}hh}$ from $t\bar{t}hh$ at FCC-hh

- Unlike many di-Higgs processes, in $t\bar{t}hh$ cross-section increases with $\lambda > \lambda_{\rm SM}$
- For κ_λ, growth of cross-section for $\lambda < 0$ has different features at 14 TeV and 100 TeV machines
- In linear EFT scenarios, the coupling modifying *ggh* and *gghh* are correlated
  $\rightarrow$ In non-linear EFT they are uncorrelated
- We vary κ_λ and $\kappa_{t\bar{t}hh}$ to obtain bounds on these couplings

Constraining κ_λ and $\kappa_{t\bar{t}hh}$ from $t\bar{t}hh$ at FCC-hh

[SB, F. Krauss, M. Spannowsky; 2019]

- For $\kappa_\lambda = 1$, $\sigma_{t\bar{t}hh}^{100\ \mathrm{TeV}}/\sigma_{t\bar{t}hh}^{14\ \mathrm{TeV}} \sim 75$
- 14 TeV study yields ~ 13 signal events and $\kappa_\lambda \lesssim 2.5$ at 95% CL [Englert *et. al.*; 2014]
- For the 100 TeV analysis, we consider final state with 6 b-tagged jets, 1 isolated lepton, at least 2 light jets and $\not{E}_T$
- Several backgrounds at play, *viz.*, QCD processes: $t\bar{t}b\bar{b}b\bar{b}$, $t\bar{t}hb\bar{b}$, $t\bar{t}Zb\bar{b}$ and EW processes $t\bar{t}hZ$, $t\bar{t}ZZ$
- Fake backgrounds: $t\bar{t}b\bar{b}+$ jets, $t\bar{t}h+$ jets, $t\bar{t}Z+$ jets, $W^\pm b\bar{b}b\bar{b}+$ jet, $W^\pm c\bar{c}c\bar{c}+$ jets, $W^\pm b\bar{b}+$ jets, $t\bar{t}c\bar{c}c\bar{c}$, misidentifying c or light jets as b-tagged jets
- We assume b-tagging efficiency of 80%, 10% (1%) mistagging efficiency for c-jets (light jets)

$t\bar{t}hh$ Scale choices

Process category	μ_F^2	μ_R^2
$t\bar{t}HH$, $t\bar{t}ZZ$, $t\bar{t}HZ$	$\frac{1}{4}\ H_T^2 + 2m_t^2 + \{2m_H^2, 2m_Z^2, m_H^2 + m_Z^2\}$	$\frac{1}{4}\ H_T^2 + 2m_t^2$
$t\bar{t}Hb\bar{b}$, $t\bar{t}Zb\bar{b}$	$\frac{1}{4}\ H_T^2 + m_{H,Z}^2 + 2m_t^2$	$\frac{1}{4}\ H_T^2 + 2m_t^2$
$t\bar{t}$ + b's, c's or light jets	$\frac{1}{4}\ H_T^2 + 2m_t^2$	$\frac{1}{4}\ H_T^2 + 2m_t^2$
W + b's, c's or light jets	$\frac{1}{4}\ H_T^2 + m_W^2$	$\frac{1}{4}\ H_T^2$

Table: Renormalisation and factorisation scales used for the various processes

Constraining κ_λ and $\kappa_{t\bar{t}hh}$ from $t\bar{t}hh$ at FCC-hh

- For the $t\bar{t}Z/h+$ jets, we consider a merged sample, where additional jets ensue from QCD radiation including the $g \to b\bar{b}$ splitting
- We ensure that the additional jets do not contain > 1 B-mesons by requiring that the B-hadron closest to the jet axis satisfies $x_B = \frac{|\vec{p}_B|}{|\vec{p}_j|} \times \frac{\vec{p}_B \cdot \vec{p}_j}{|\vec{p}_B||\vec{p}_j|} > 0.7$
- Reflects b-quark fragmentation $\to$ Allows to suppress "doubly-tagged" b-jets
- We first reconstruct the two Higgs bosons by minimising the following χ^2

$$\chi^2_{HH} = \frac{(m_{b_i,b_j} - m_h)^2}{\Delta_h^2} + \frac{(m_{b_k,b_l} - m_h)^2}{\Delta_h^2},$$

  $i \neq j \neq k \neq l$ run over all the 6 b-tagged jets, $m_h = 120$ GeV taking into account invisible decays of B-mesons and $\Delta_h = 20$ GeV
- We then require require $|m_{b_i,b_j} - m_h| < \Delta_h$ and $|m_{b_k,b_l} - m_h| < \Delta_h$

Constraining κ_λ and $\kappa_{t\bar{t}hh}$ from $t\bar{t}hh$ at FCC-hh

- Then we take the 2 remaining b-jets and minimise the following χ^2

$$\chi^2_{t_h} = \frac{(m_{b_i,j_k,j_l} - m_t)^2}{\Delta_t^2},$$

$k \neq l$ and $\Delta_t = 40$ GeV We then require $|m_{b_i,j_k,j_l} - m_t| < \Delta_t$

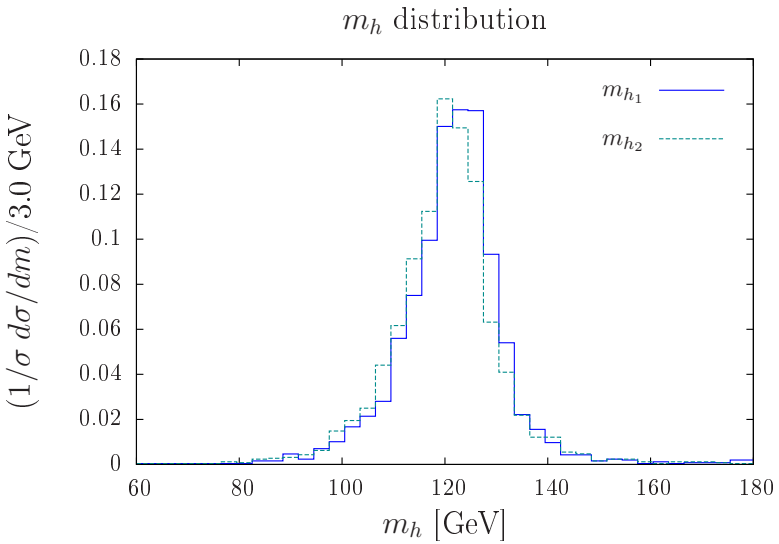

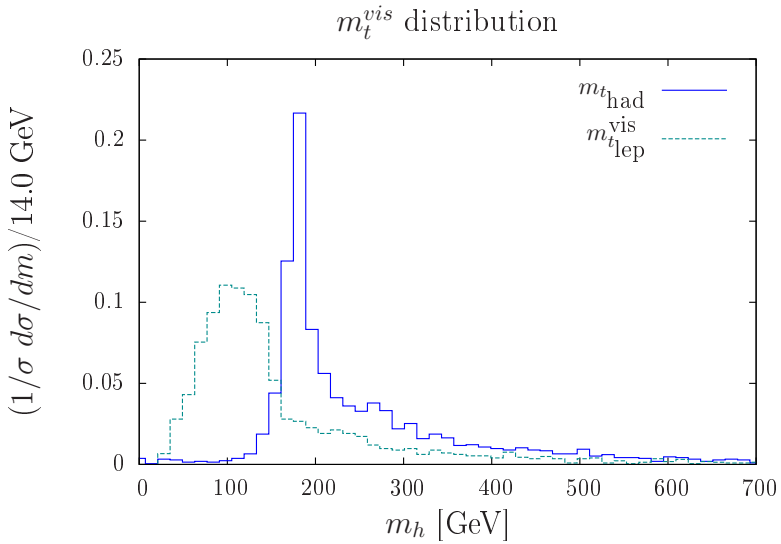

- Finally we require $m^{vis}_{t_{lep}} < m_t$

Constraining κ_λ and $\kappa_{t\bar{t}hh}$ from $t\bar{t}hh$ at FCC-hh

[SB, F. Krauss, M. Spannowsky; 2019]

- At the design luminosity of 30 ab^{-1}, we expect ~ 260 signal events for $\kappa_\lambda = 1$ and ~ 1900 background events, with $S/B \sim 0.14$ and statistical significance of $S/\sqrt{B} \sim 5.9$
- Upon taking $\kappa_{t\bar{t}hh} = 0$, one obtains (using the CLs method) at 68% CL with 5% (10%) systematic uncertainty

$$-3.20 < \kappa_\lambda < 2.60 \; (-3.43 < \kappa_\lambda < 2.92) \quad 3/\mathrm{ab}$$

$$-2.89 < \kappa_\lambda < 2.15 \; (-3.27 < \kappa_\lambda < 2.70) \quad 30/\mathrm{ab}$$

- Upon taking $\kappa_\lambda = 1$, one obtains (using the CLs method) at 68% CL with 5% (10%) systematic uncertainty

$$-0.59 \; \mathrm{TeV}^{-1} < \kappa_{t\bar{t}hh} < 0.95 \; \mathrm{TeV}^{-1} \; (-0.71 \; \mathrm{TeV}^{-1} < \kappa_{t\bar{t}hh} < 1.07 \; \mathrm{TeV}^{-1}) \quad 3/\mathrm{ab}$$

$$-0.43 \; \mathrm{TeV}^{-1} < \kappa_{t\bar{t}hh} < 0.78 \; \mathrm{TeV}^{-1} \; (-0.63 \; \mathrm{TeV}^{-1} < \kappa_{t\bar{t}hh} < 0.99 \; \mathrm{TeV}^{-1}) \quad 30/\mathrm{ab}$$

- Ultimate goal is to perform a global fit using the $pp \to hh$, $pp \to hhj$, $pp \to hhjj$ and $pp \to t\bar{t}hh$ with all these couplings to find correlated bounds

Resonant di-Higgs at HL-LHC and FCC-hh

- Bounds on $\sigma(pp \to H \to hh)$ at HL-LHC (left) from various channels and at FCC-hh (right) from $b\bar{b}b\bar{b}$
  [A. Adhikary, SB, R. K. Barman and B. Bhattacherjee; 2018, D. Barducci, K. Mimasu, J. M. No, C. Vernieri and J. Zurita; 2019]

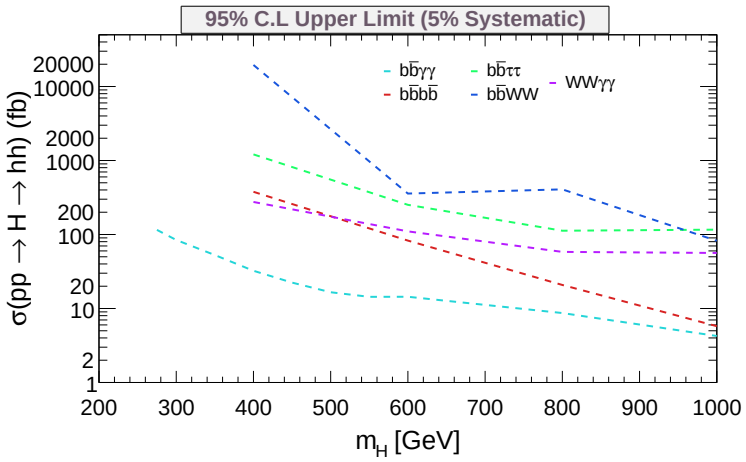

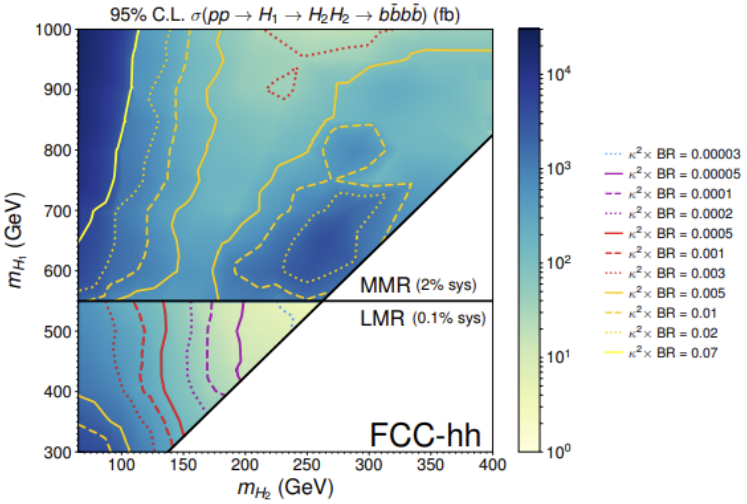

- Right plot: isocontours of sensitivity on $\kappa^2 \times \mathrm{BR}$ ($\kappa^2 \times \mathrm{BR}$ is defined by $\sigma\left(pp \to H_1 \to H_2 H_2 \to b\bar{b}b\bar{b}\right) = \hat{\sigma}_{H_1} \times \kappa^2 \times \mathrm{BR}$ and $\hat{\sigma}_{H_1}$ is production of SM-like Higgs with mass m_{H_1})
- FCC-hh can set stringent limit on $\kappa \times \mathrm{BR} \to$ factor ~ 40 improvement with respect to HL-LHC

Summary and Outlook

- Search for Higgs pair production is an important enterprise to understand the Higgs cubic coupling
- Non-resonant di-Higgs searches at the HL-LHC yields a significance of $\sim 3\sigma$
- 100 TeV collider studies show promise for di-Higgs + jet $\rightarrow \kappa_\lambda$ can be constrained to $\sim 8\%$
- Possible to disentangle $\kappa_{t\bar{t}hh}$ and κ_λ by combining $pp \rightarrow hh, pp \rightarrow hhj$ and $pp \rightarrow hhjj$ with $pp \rightarrow t\bar{t}hh$. Also other final states in $pp \rightarrow t\bar{t}hh$.
- Possible to constrain λ_{hhhh} from one loop EW correction to $t\bar{t}hh$ at FCC-hh [SB, J. Lindert; ongoing]
- Systematic uncertainties need to be understood better in the future in order to make strong claims about these channels
- A global analysis with several di-Higgs channels will ultimately shed light on the couplings of the scalar sector and with the scalar and the top-quarks

Backup slides

Non resonant di-Higgs production at the HL-LHC: $b\bar{b}\gamma\gamma$

[A. Adhikary, SB, R. K. Barman, B. Bhattacherjee, S. Niyogi; 2017]

- Cleanest channel in spite of the low rate
- Major backgrounds: QCD-QED $b\bar{b}\gamma\gamma$, $hb\bar{b}$, $t\bar{t}h$, Zh
- Dominant fakes: $c\bar{c}\gamma\gamma$, $jj\gamma\gamma$, $b\bar{b}j\gamma$, $c\bar{c}j\gamma$, $b\bar{b}jj$

Selection cuts
$N_j < 6$
$0.4 < \Delta R_{\gamma\gamma} < 2.0,\ 0.4 < \Delta R_{bb} < 2.0,\ \Delta R_{\gamma b} > 0.4$
$100\ \mathrm{GeV} < m_{bb} < 150\ \mathrm{GeV}$
$122\ \mathrm{GeV} < m_{\gamma\gamma} < 128\ \mathrm{GeV}$
$p_{T,bb} > 80\ \mathrm{GeV},\ p_{T,\gamma\gamma} > 80\ \mathrm{GeV}$

Cut flow	Event rates with 3000 fb^{-1} of integrated luminosity							$\frac{S}{\sqrt{B}}$
	Signal	SM Backgrounds						
	$hh \to 2b2\gamma$	$hb\bar{b}$	$t\bar{t}h$	Zh	$b\bar{b}\gamma\gamma^*$	Fake 1	Fake 2	
Order	NNLO	NNLO (5FS) + NLO (4FS)	NLO	NNLO (QCD) + NLO EW	LO	LO	LO	
$2b + 2\gamma$	31.63	21.20	324.91	39.32	25890.31	1141.18	393.79	0.19
lepton veto	31.63	21.20	255.66	39.32	25889.94	1141.18	393.79	0.19
$N_j < 6$	31.04	21	192.05	39.23	25352.78	1064.64	167.32	0.19
ΔR cuts	22.19	7.75	38.71	23.48	4715.21	130.10	28.81	0.31
m_{bb}	12.71	1.53	13.80	1.09	862.37	22.11	6.88	0.42
$m_{\gamma\gamma}$	12.36	1.5	13.16	1.06	26.54	22.11	6.88	1.46
$p_{T,bb}, p_{T,\gamma\gamma}$	12.32	1.48	13.03	1.06	26.54	21.82	6.88	1.46

- significance: $S/B = 0.17$ and $S/\sqrt{B} = 1.46$
- With additional $\not{E}_T < 50$ GeV, $S/B = 0.19$ and $S/\sqrt{B} = 1.51$
- Changing to: 90 GeV $< m_{bb} <$ 130 GeV: $S/B = 0.19$ and $S/\sqrt{B} = 1.64$
- $b\bar{b}\gamma\gamma^* = b\bar{b}\gamma\gamma + c\bar{c}\gamma\gamma + jj\gamma\gamma$, Fake1 $= b\bar{b}j\gamma + c\bar{c}j\gamma$, Fake2 $= b\bar{b}jj$

- Multivariate technique employed to further optimise search
- Boosted decision tree (BDT) algorithms chosen
- Overtaining checked using the Kolmogorov-Smirnov test
- Variables chosen (according to the best discriminatory power):

$$m_{bb},\ p_{T,\gamma\gamma},\ \Delta R_{\gamma\gamma},\ p_{T,bb},\ \Delta R_{b_1\gamma_1},\ p_{T,\gamma_1},\ \Delta R_{bb},$$
$$p_{T,\gamma_2},\ \Delta R_{b_2\gamma_1},\ \Delta R_{b_2\gamma_2},\ p_{T,b_1},\ \Delta R_{b_1\gamma_2},\ p_{T,b_2},\ \not{E}_T$$

- $S/B = 0.19$ and $S/\sqrt{B} = 1.76\sigma$ CMS (ATLAS) projection: 1.6σ (1.05σ)

Non resonant di-Higgs production at the HL-LHC: $b\bar{b}WW^*$

- Two scenarios considered: leptonic: $b\bar{b}\ell\ell + \not{E}_T$ and semi-leptonic: $b\bar{b}\ell jj + \not{E}_T$
- Major backgrounds: $t\bar{t}$: leptonic and semi-leptonic, $Wb\bar{b}+$ jets: semi-leptonic, $\ell\ell bb$: leptonic and semi-leptonic
- Subdominant backgrounds: $b\bar{b}h$, $t\bar{t}h$, $t\bar{t}V$, Vh, $Vb\bar{b}$, VVV: leptonic and semi-leptonic
- Variables for $b\bar{b}\ell\ell + \not{E}_T$

$$p_{T,\ell_{1/2}},\ \not{E}_T,\ m_{\ell\ell},\ m_{bb},\ \Delta R_{\ell\ell},\ \Delta R_{bb},\ p_{T,bb},\ p_{T,\ell\ell},\ \Delta\phi_{bb\,\ell\ell},$$

- Variables for $b\bar{b}\ell jj + \not{E}_T$

$$p_{T,\ell},\ \not{E}_T,\ m_{jj},\ m_{bb},\ \Delta R_{jj},\ \Delta R_{bb},\ p_{T,bb},\ p_{T,\ell jj},\ \Delta\phi_{bb\,\ell jj},\ \Delta R_{\ell\,jj},$$

Limits on κ_λ from $hh \to b\bar{b}\gamma\gamma$: Various hypotheses

[A. Adhikary, SB, R. K. Barman, B. Bhattacherjee, S. Niyogi; 2017]

- Our results corroborate with ATLAS' HL-LHC predictions

$-0.86 < \kappa_\lambda < 7.96$	CBA for $\kappa_\lambda = 1$ optimisation; SM null hypothesis
$-0.63 < \kappa_\lambda < 8.07$	BDT analysis for $\kappa_\lambda = 1$ optimisation; SM null hypothesis
$-0.81 < \kappa_\lambda < 6.06$	BDT analysis for $\kappa_\lambda = 5$ optimisation; SM null hypothesis
$-1.24 < \kappa_\lambda < 6.49$	BDT analysis for $\kappa_\lambda = 5$ optimisation; $\kappa = 5$ null hypothesis.

Non resonant di-Higgs production at the HL-LHC: $b\bar{b}\tau^+\tau^-$

- Major backgrounds: $t\bar{t}$ (hadronic, semi-leptonic and leptonic), $\ell\ell b\bar{b}$, $hb\bar{b}$, Zh, $t\bar{t}X$, $b\bar{b}jj$
- Variables for $\tau_h\tau_h$, $\tau_h\tau_\ell$ and $\tau_\ell\tau_\ell$:

$$p_{T,bb},\ m_{bb},\ \Delta R_{bb},\ M_{\tau_h\tau_h},\ m_{T2},\ \Delta\phi_{\tau_{h_1}\not{E}_T},\ m_{hh}^{\rm vis},\ p_{T,hh}^{\rm vis},\ \Delta R_{hh}^{\rm vis}$$

$$p_{T,bb},\ m_{bb},\ \Delta R_{bb},\ M_{\tau_h\tau_l},\ m_{T2},\ \Delta\phi_{\tau_h\not{E}_T},\ \Delta\phi_{\tau_\ell\not{E}_T},\ m_{hh}^{\rm vis},\ \Delta R_{hh}^{\rm vis}$$

$$p_{T,bb},\ m_{bb},\ \Delta R_{bb},\ M_{\tau_l\tau_l},\ m_{T2},\ \Delta\phi_{\tau_{\ell_1}\not{E}_T},\ \Delta\phi_{\tau_{\ell_2}\not{E}_T},\ m_{hh}^{\rm vis}$$

- $\tau_h\tau_h$: $S/B = 0.013$, $S/\sqrt{B} = 0.74$; $\tau_h\tau_\ell$: $S/\sqrt{B} = 0.49$; $\tau_\ell\tau_\ell$: $S/\sqrt{B} = 0.08$

Non resonant di-Higgs production at the HL-LHC: $b\bar{b}\tau^+\tau^-$

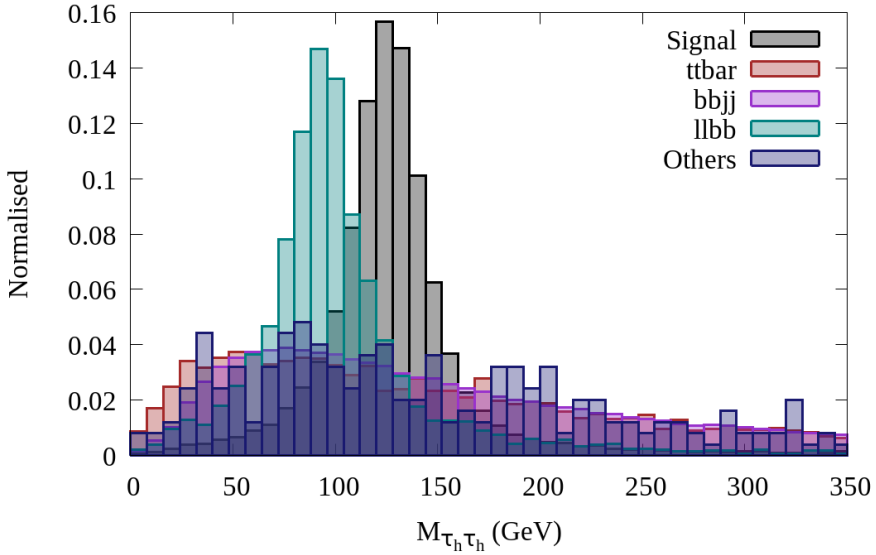

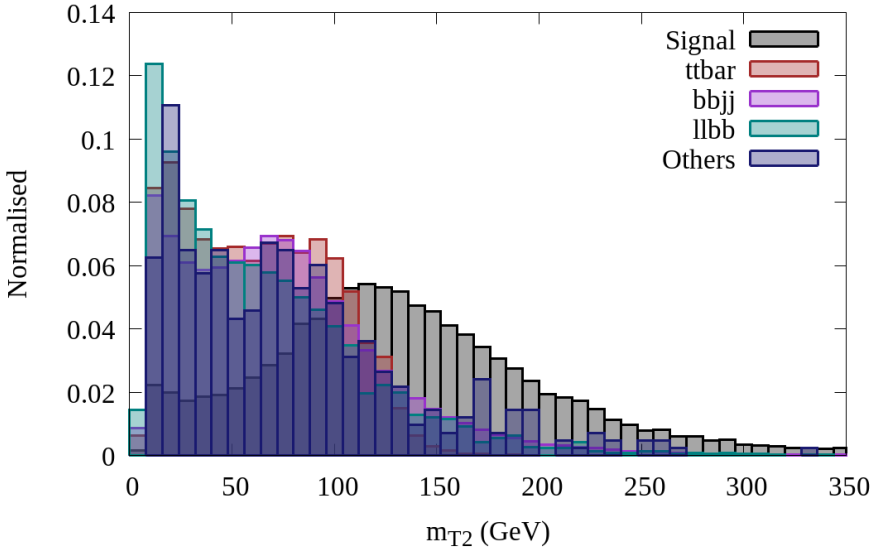

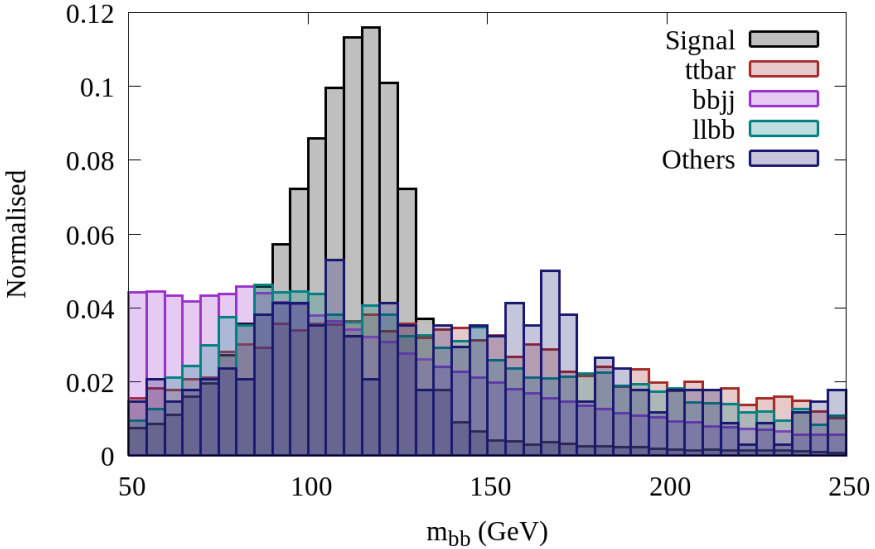

Non resonant di-Higgs production at the HL-LHC: $b\bar{b}WW^*$

- Semi-leptonic: $S/B = 1.2 \times 10^{-4}$ and $S/\sqrt{B} = 0.13$

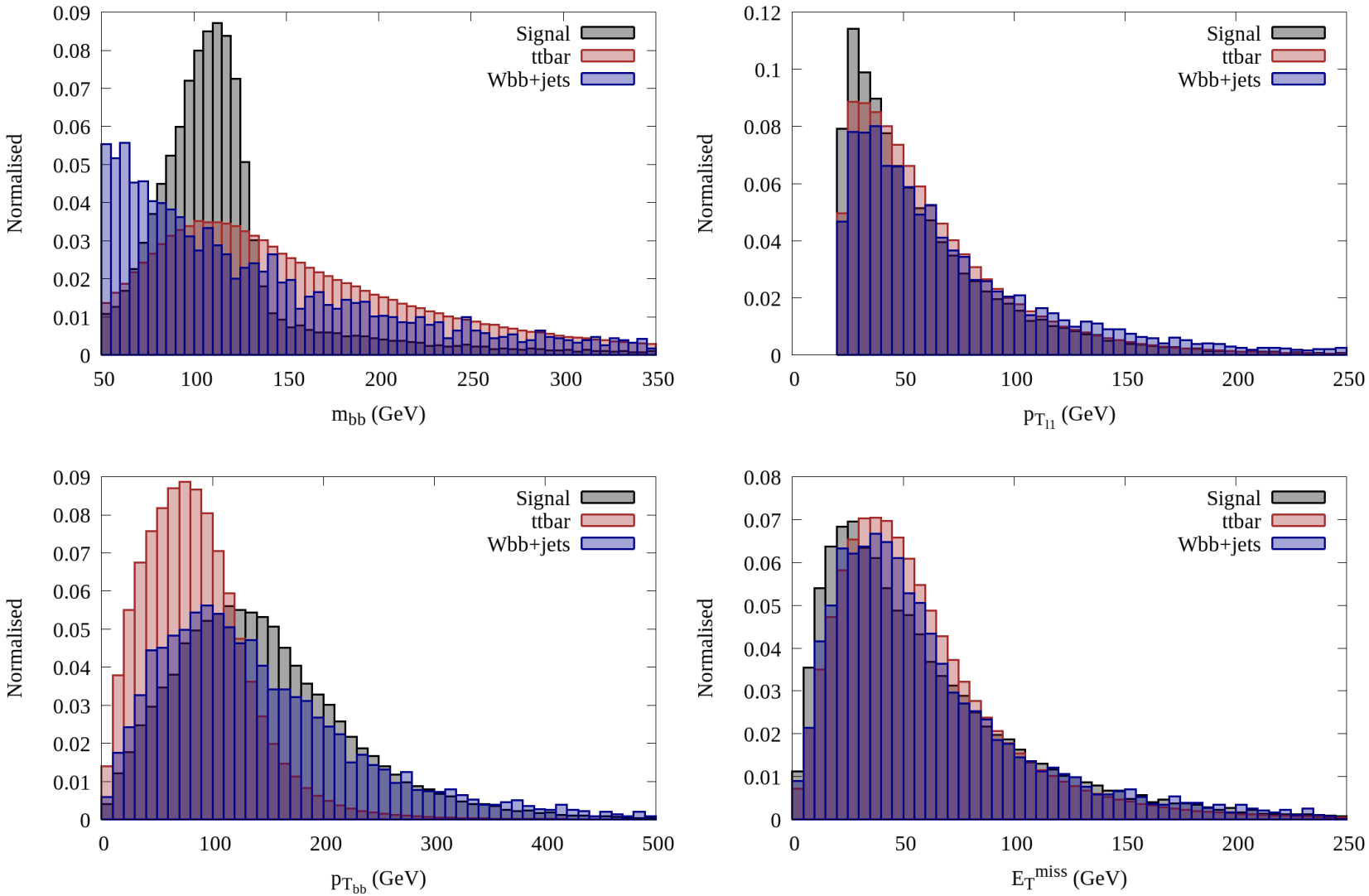

Non resonant di-Higgs production at the HL-LHC: $\gamma\gamma WW^*$

- We study fully leptonic: $\ell^+\ell^-\gamma\gamma + \not{E}_T$ and semi-leptonic: $\ell jj\gamma\gamma + \not{E}_T$ states
- Fully hadronic case entails an enormous background
- Backgrounds: $t\bar{t}h$, $Zh +$ jets, $\ell\ell\gamma\gamma +$ jets (leptonic) and $Wh +$ jets, $\ell\nu\gamma\gamma +$ jets (in addition for semi-leptonic case)
- In addition demand b-jet veto to control the $t\bar{t}h$ backgrounds
- Variables for $\ell^+\ell^-\gamma\gamma + \not{E}_T$

$$p_{T,\ell_{(1,2)}},\ \not{E}_T,\ m_{\ell\ell},\ m_{\gamma\gamma},\ \Delta R_{\gamma\gamma(\ell\ell)},\ p_{T,\ell\ell},\ p_{T,\gamma\gamma},\ \Delta\phi_{\ell\ell\,\gamma\gamma}$$

- Variables for $\ell jj\gamma\gamma + \not{E}_T$

$$p_{T,\ell_1},\ \not{E}_T,\ m_{\gamma\gamma},\ \Delta R_{\gamma\gamma},\ p_{T,\gamma\gamma},\ p_{T,\ell j},\ \Delta\phi_{\ell j\,\gamma\gamma},\ \Delta R_{\ell j},\ m_T$$

Non resonant di-Higgs production at the HL-LHC: $\gamma\gamma WW^*$

- Leptonic: $S/B = 0.40$; Less than 1 signal event; Higher luminosity/energy

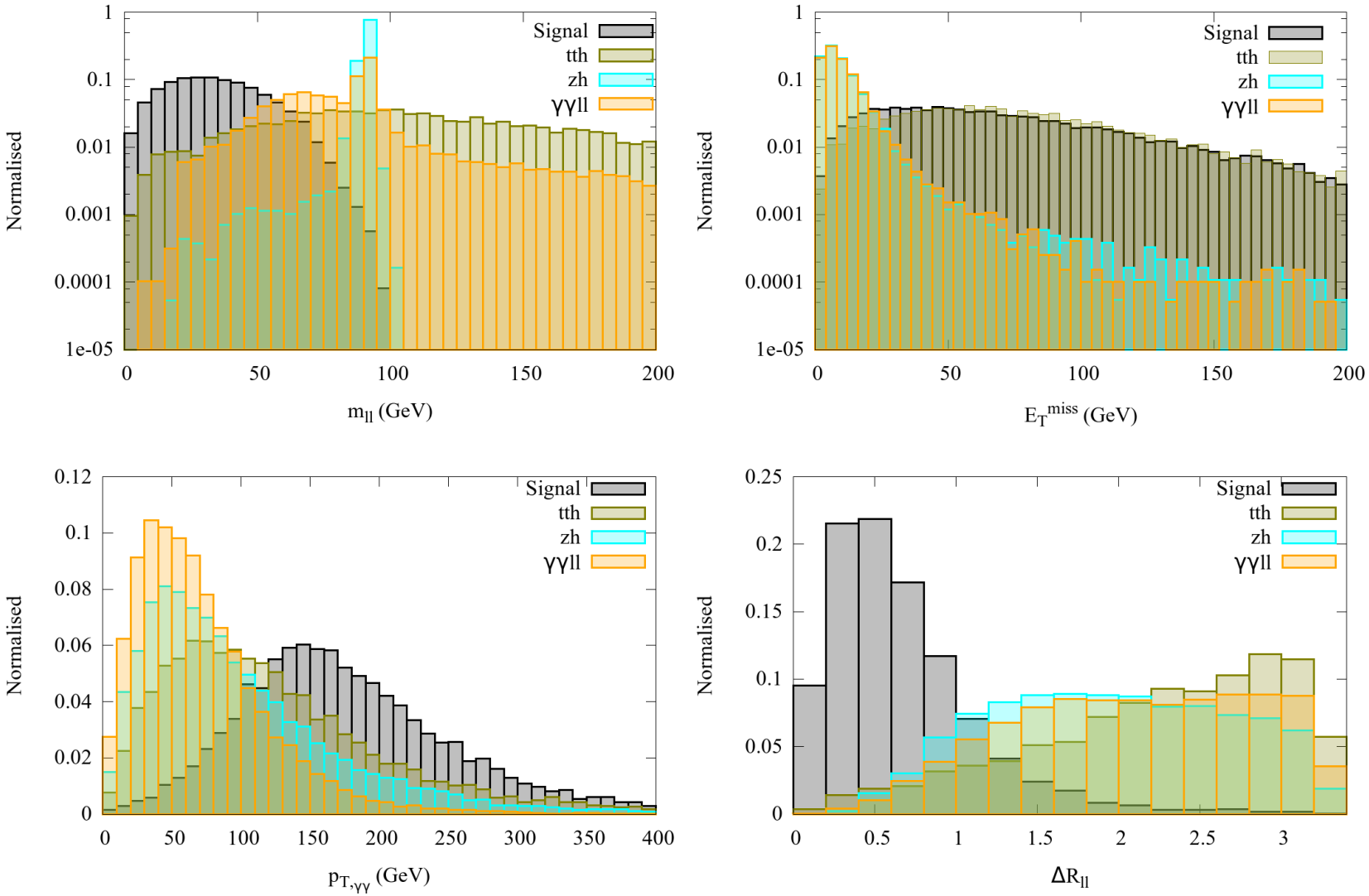

Non resonant di-Higgs production at the HL-LHC: $\gamma\gamma WW^*$

- Semi-leptonic: $S/B = 0.11$; Less than 5 signal events; Higher luminosity/energy: Perfect channel at 100 TeV colliders

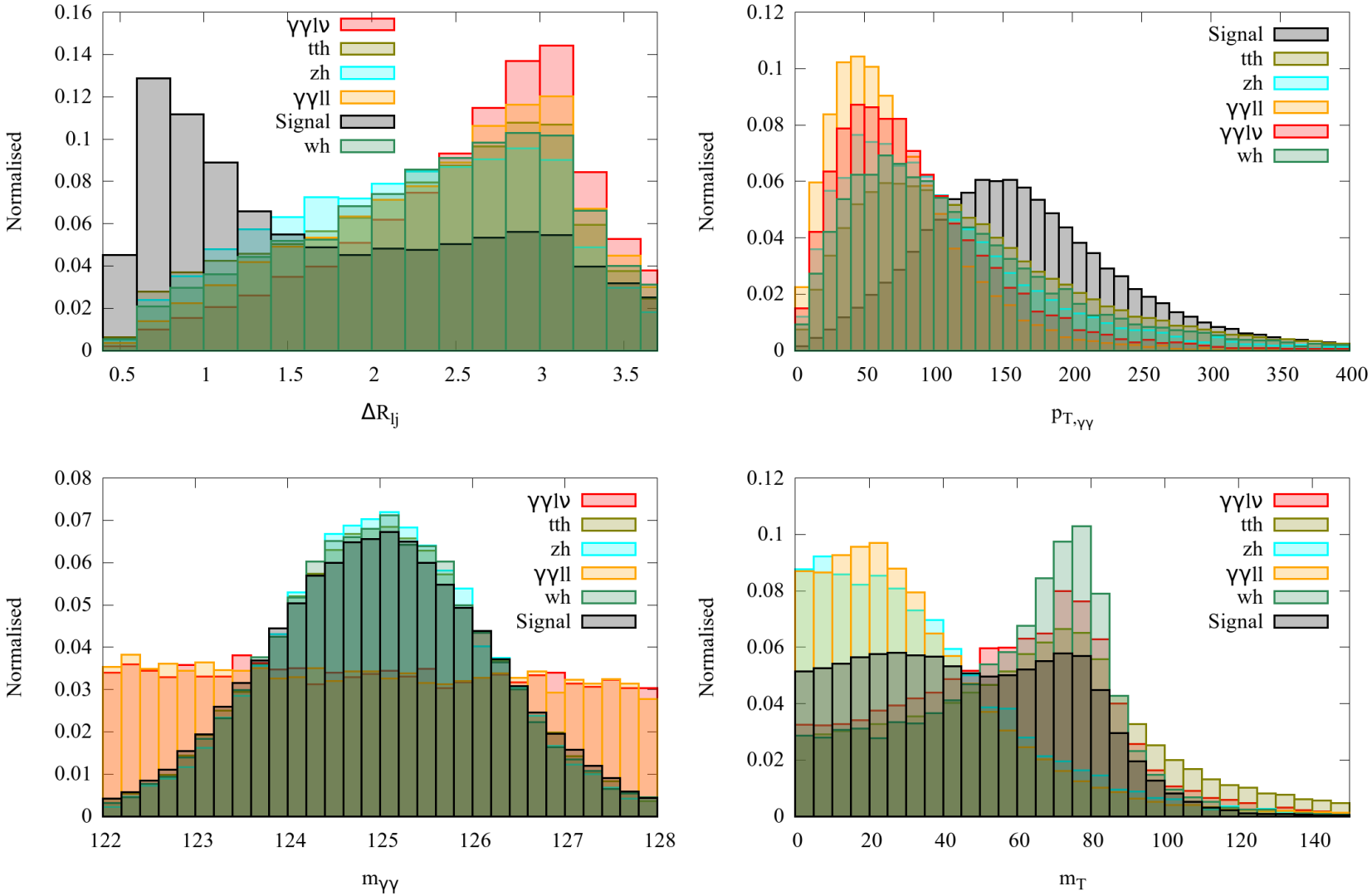

Non resonant di-Higgs production at the HL-LHC: $4W$

- We consider $\ell^\pm\ell^\pm + 4j + \not{E}_T$ ($SS2\ell$), $3\ell + 2j + \not{E}_T$ (3ℓ) and $4\ell + \not{E}_T$ (4ℓ)
- Lose cleanliness (rate) upon including more jets (leptons)
- Major backgrounds for $SS2\ell$: WZ, $t\bar{t}$, $W^\pm W^\pm$, Vh, $t\bar{t}X$, VVV, 4ℓ
- For $SS2\ell$, demand two same-sign leptons with $p_T > 25$ GeV and at least two jets with $p_T > 30$ GeV
- Major backgrounds for 3ℓ: Same as before save for $W^\pm W^\pm$
- For 3ℓ, $p_{T,\ell_{1/2/3}} > 25, 20, 15$ GeV and $|m_Z - m_{\ell\ell}| > 20$ GeV
- Variables for $SS2\ell$

$$m_{\ell^\pm\ell^\pm},\ \Delta R_{\ell_i j_k},\ m_{jj}$$

- Variables for 3ℓ

$$m_{\ell_i\ell_j},\ \Delta R_{\ell_i\ell_j},\ m_{\ell\ell\ell},\ m_{\rm eff},\ \not{E}_T,\ p_{T,\ell_i},\ n_{\rm jet}$$

Non resonant di-Higgs production at the HL-LHC: $4W$

- $SS2\ell$: $S/B = 1 \times 10^{-3}$, $S/\sqrt{B} = 0.11$

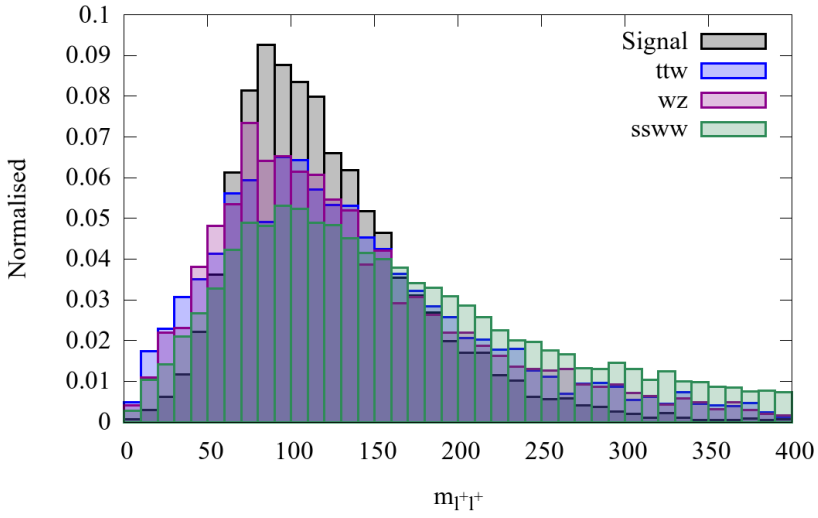

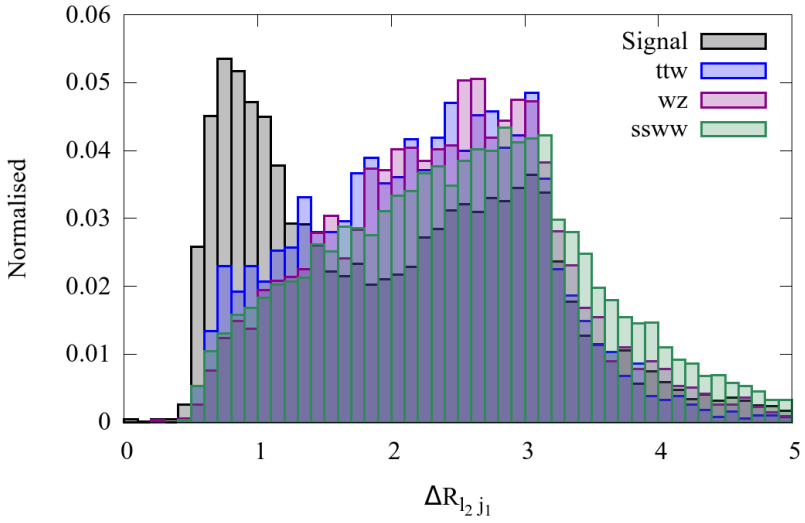

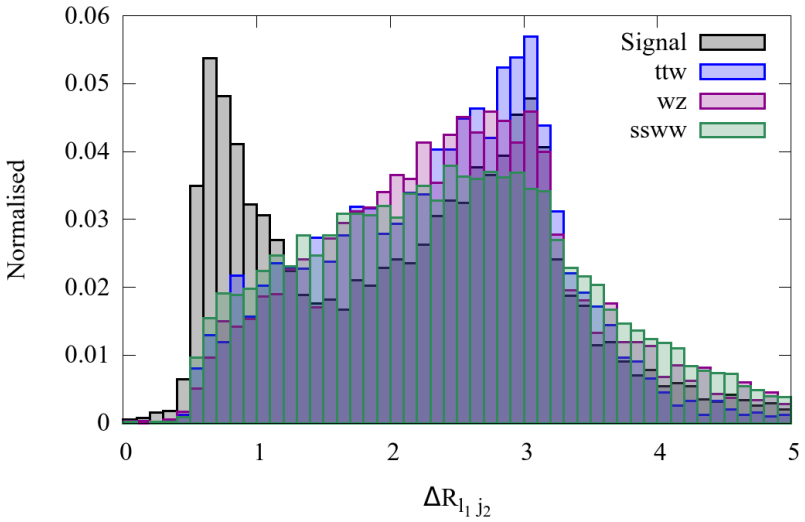

Non resonant di-Higgs production at the HL-LHC: $4W$

- 3ℓ: $S/B = 3 \times 10^{-3}$, $S/\sqrt{B} = 0.20$

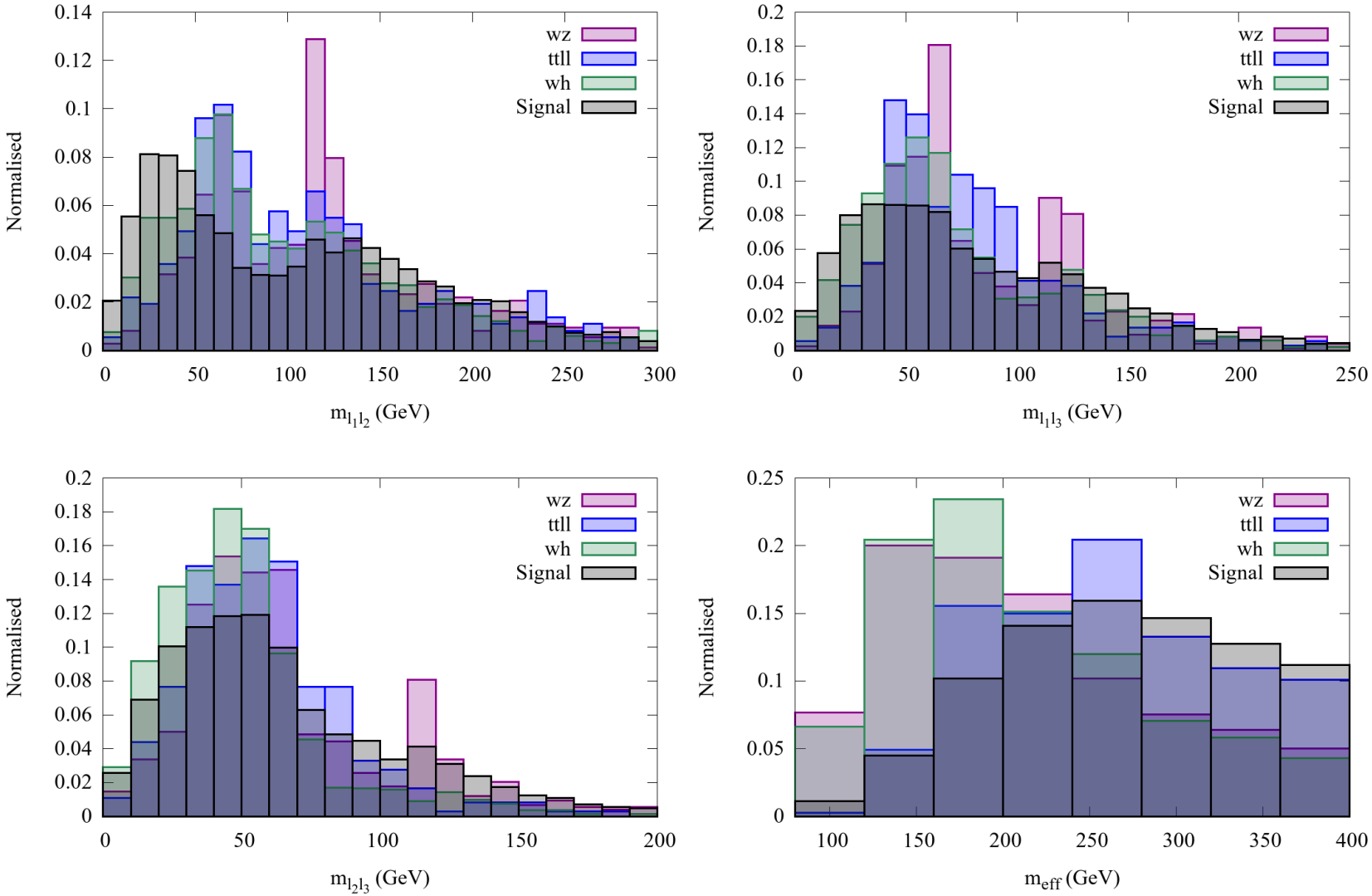

Machinery in a nutshell

- Di-Higgs samples and backgrounds generated at LO with `MG5_aMC@NLO`
- Signal samples decayed using `Pythia-6`
- NN23LO parton distribution function employed
- Default factorisation and renormalisation scales used
- Shower + hadronisation using `Pythia-6`
- `Delphes-3.4.1` used for detector simulation
- Jets: anti-kT algorithm, $p_T > 20$ GeV, $R = 0.4$ (`FastJet`)
- Total energy around e, μ, γ required to be $< 12\%, 25\%, 12\%$ within $\Delta R = 0.5$
- b-tag efficiency: 70%, $j \to b$: 1%, $c \to b$: 30%

m_{T2}

- Dominant $t\bar{t}$ background can be greatly tackled with this variable
- Designed for the case where a pair of equal mass particles (A and A') decay : $A \to B + C$, $A' \to B' + C'$
- B and B' are visible particles and C and C' are not observed
- m_{T2} gives the maximal possible mass of parent particle A; provides greatest lower bound on $m_A = m_{A'}$
- $m_{T2}(m_B, m_{B'}, \mathbf{b}_T, \mathbf{b}_{T'}, \mathbf{p_T}^{\Sigma}, m_C, m_{C'}) \equiv \min_{\mathbf{c}_T + \mathbf{c}_{T'} = \mathbf{p}_T^{\Sigma}} \{max(m_T, m_{T'})\}$
- $m_T^2(\mathbf{b}_T, \mathbf{c}_T, m_b, m_c) \equiv m_b^2 + m_c^2 + 2(e_b e_c - \mathbf{b}_T \cdot \mathbf{c}_T)$, with $e^2 = m^2 + \mathbf{p}_T^2$
- Bounded above by top mass but unbounded below for the di-Higgs process

BDRS

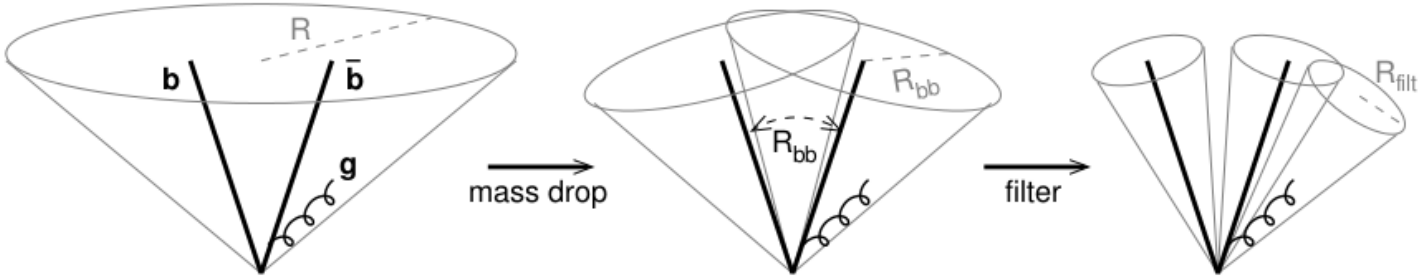

FIG. 1: The three stages of our jet analysis: starting from a hard massive jet on angular scale R, one identifies the Higgs neighbourhood within it by undoing the clustering (effectively shrinking the jet radius) until the jet splits into two subjets each with a significantly lower mass; within this region one then further reduces the radius to $R_{\rm filt}$ and takes the three hardest subjets, so as to filter away UE contamination while retaining hard perturbative radiation from the Higgs decay products.

Given a hard jet j, obtained with some radius R, we then use the following new iterative decomposition procedure to search for a generic boosted heavy-particle decay. It involves two dimensionless parameters, μ and $y_{\rm cut}$:

1. Break the jet j into two subjets by undoing its last stage of clustering. Label the two subjets j_1, j_2 such that $m_{j_1} > m_{j_2}$.
2. If there was a significant mass drop (MD), $m_{j_1} < \mu m_j$, and the splitting is not too asymmetric, $y = \frac{\min(p^2_{tj_1}, p^2_{tj_2})}{m_j^2} \Delta R^2_{j_1,j_2} > y_{\rm cut}$, then deem j to be the heavy-particle neighbourhood and exit the loop. Note that $y \simeq \min(p_{tj_1}, p_{tj_2}) / \max(p_{tj_1}, p_{tj_2})$.[1]
3. Otherwise redefine j to be equal to j_1 and go back to step 1.

The final jet j is to be considered as the candidate Higgs boson if both j_1 and j_2 have b tags. One can then identify $R_{b\bar{b}}$ with $\Delta R_{j_1 j_2}$. The effective size of jet j will thus be just sufficient to contain the QCD radiation from the

In practice the above procedure is not yet optimal for LHC at the transverse momenta of interest, $p_T \sim 200 - 300\,\text{GeV}$ because, from eq. (1), $R_{b\bar{b}} \gtrsim 2m_{\rm H}/p_T$ is still quite large and the resulting Higgs mass peak is subject to significant degradation from the underlying event (UE), which scales as $R^4_{b\bar{b}}$ [15]. A second novel element of our analysis is to *filter* the Higgs neighbourhood. This involves resolving it on a finer angular scale, $R_{\rm filt} < R_{b\bar{b}}$, and taking the three hardest objects (subjets) that appear — thus one captures the dominant $\mathcal{O}(\alpha_s)$ radiation from the Higgs decay, while eliminating much of the UE contamination. We find $R_{\rm filt} = \min(0.3, R_{b\bar{b}}/2)$ to be rather effective. We also require the two hardest of the subjets to have the b tags.

N-Subjettines: Backup

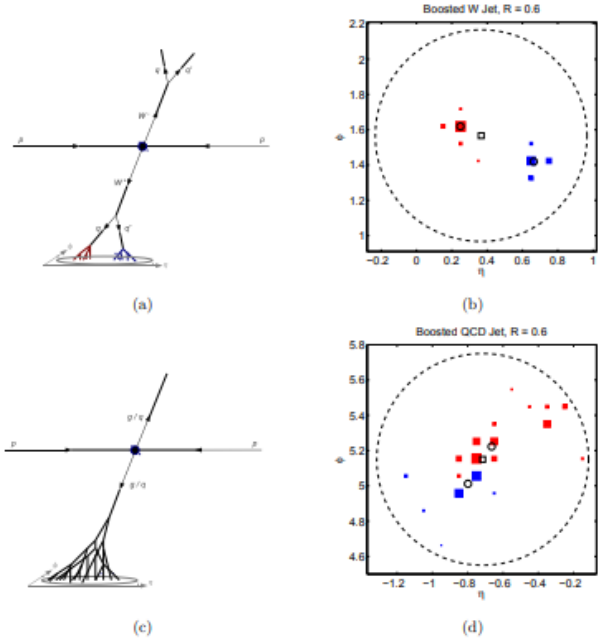

Figure 1: Left: Schematic of the fully hadronic decay sequences in (a) W^+W^- and (c) dijet QCD events. Whereas a W jet is typically composed of two distinct lobes of energy, a QCD jet acquires invariant mass through multiple splittings. Right: Typical event displays for (b) W jets and (d) QCD jets with invariant mass near m_W. The jets are clustered with the anti-k_T jet algorithm [31] using $R = 0.6$, with the dashed line giving the approximate boundary of the jet. The marker size for each calorimeter cell is proportional to the logarithm of the particle energies in the cell. The cells are colored according to how the exclusive k_T algorithm divides the cells into two candidate subjets. The open square indicates the total jet direction and the open circles indicate the two subjet directions. The discriminating variable τ_2/τ_1 measures the relative alignment of the jet energy along the open circles compared to the open square.

$t\bar{t}hh$ cross-sections: Backup

Channel	Cross-section [pb]
$t\bar{t}hh$ ($\kappa_\lambda = 1$)	0.016
$t\bar{t}hh$ ($\kappa_\lambda = 2$)	0.022
$t\bar{t}hh$ ($\kappa_\lambda = 0$)	0.014
$t\bar{t}hh$ ($\kappa_\lambda = -1$)	0.013
$t\bar{t}hh$ ($\kappa_\lambda = -2$)	0.015
$t\bar{t}hh$ ($\kappa_{t\bar{t}hh} = -0.003$)	0.175
$t\bar{t}hh$ ($\kappa_{t\bar{t}hh} = 0.003$)	0.132
$t\bar{t}b\bar{b}b\bar{b}$	0.174
$t\bar{t}c\bar{c}c\bar{c}$	0.174
$t\bar{t}b\bar{b}$+jets	46.30
$t\bar{t}hb\bar{b}$	0.076
$t\bar{t}h$+jets	12.825
$t\bar{t}hZ$	0.045
$t\bar{t}ZZ$	0.057
$t\bar{t}Zb\bar{b}$	0.165
$t\bar{t}Z$+jets	25.663
$W^\pm b\bar{b}b\bar{b}$+ jet	0.036
$W^\pm c\bar{c}c\bar{c}$+ jet	0.092

Table: Table shows the generation level cross-sections for the signal and background processes. We require the Higgs bosons to decay to a pair of b/c quarks, the Z-bosons to all quarks. Furthermore, we require the $W^\pm$-bosons to decay leptonically. These branching ratios are included in these cross-sections. For the signals, κ_λ, is the ratio of the Higgs self-coupling to the SM value and $\kappa_{t\bar{t}hh}$ is the coupling of the four point $t\bar{t}hh$ interaction. The processes with b/c quarks in the final state in the matrix element level have a further requirement of $m_{bb/cc/bc} > 50$ GeV, $p_T(b/c) > 25$ GeV, D-parameter > 0.4, $|y| < 4.0$.